HHS Public Access

Author manuscript

Oncogene. Author manuscript; available in PMC 2012 October 19.

Published in final edited form as:

Oncogene. 2012 April 19; 31(16): 2028–2038. doi:10.1038/onc.2011.385.

Different Phenotypic Consequences of Simultaneous Versus Stepwise *Apc* Loss

Jared M Fischer, PhD[1], **Ashleigh J Miller, PhD**[1], **Darryl Shibata, MD**[2], and **R Michael Liskay, PhD**[1]

[1]Molecular and Medical Genetics, Oregon Health and Science University, 3181 Sam Jackson Park Road, Portland, OR, 97239

[2]Department of Pathology, Norris Cancer Center, University of Southern California School of Medicine, 1441 Eastlake Avenue, NOR 2424, Los Angeles, CA 90033

Abstract

APC is considered a gatekeeper for colorectal cancer (CRC). Cells with heterozygous *APC* mutations have altered expression profiles suggesting that the first *APC* hit may help set the stage for subsequent transformation. Therefore, we measured transformation efficiency following what we have designated as “simultaneous” versus “stepwise” *Apc* loss. We combined a conditional *Apc* allele (Apc^{CKO}) with a Cre reporter gene and an out-of-frame *Cre* allele ($Pms2^{cre}$) that stochastically becomes functional by a frameshift mutation in single cells. Loss of one *Apc* allele ($Apc^{CKO/+}$) had little consequence, whereas simultaneous loss of both *Apc* alleles ($Apc^{CKO/CKO}$) resulted in increased clonal expansion (crypt fission), consistent with the gatekeeper function of Apc. Interestingly, our analyses showed that most of the *Apc*-deficient crypts in $Apc^{CKO/CKO}$ mice appeared normal, with morphologic transformation, including β-catenin deregulation, occurring in only 17% of such crypts. To determine whether transformation efficiency was different following stepwise Apc loss, we combined Apc^{CKO} with a germline mutant allele, either Apc^{Min} or Apc^{1638N}. Transformation efficiency following stepwise *Apc* loss ($Apc^{Min/CKO}$ or $Apc^{1638N/CKO}$) was increased 5-fold and essentially all of the *Apc*-deficient cells were dysplastic. In summary, our data suggest that the gatekeeper function of Apc consists of two roles, clonal expansion and morphologic transformation, because simultaneous *Apc* loss frequently leads to occult clonal expansion without morphologic transformation, whereas stepwise *Apc* loss more often results in visible neoplasia. Finally, that *Apc*-deficient cells in certain scenarios can retain a normal phenotype is unexpected and may have clinical implications for surveillance strategies to prevent CRC.

Keywords

APC; cancer; simultaneous; stepwise; intestine

*CORRESPONDANCE: R Michael Liskay, Molecular and Medical Genetics, Oregon Health and Science University, 3181 Sam Jackson Park Road, Portland, OR, 97239, (503) 494-4346, liskaym@ohsu.edu.

CONFLICT OF INTEREST: The authors declare no conflicts of interest.

INTRODUCTION

Colorectal cancer (CRC) is thought to occur after the accumulation of mutations in multiple oncogenes and tumor suppressor genes. The order of these mutations is uncertain; however, *APC* is considered to have a gatekeeper role because its mutation is thought to initiate tumorigenesis (Fearon and Vogelstein, 1990). Germline *APC* mutations are associated with familial adenomatous polyposis (FAP), and *APC* mutations are found in the majority of adenomas (Forbes et al., 2010). Mice have been genetically manipulated with germline *Apc* mutations to mimic both FAP (Oshima et al., 1995; Sasai et al., 2000; Su et al., 1992) and attenuated FAP (Fodde et al., 1994). The gatekeeper function of *Apc* has been tested in murine models by combining a conditional *Apc* allele with an inducible *Cre* gene. Intestine-wide conditional loss of *Apc* using an epithelial-specific promoter resulted in morphologic hyperplasia within five days (Sansom et al., 2004). Loss of *Apc* in isolated $Lgr5^+$ stem cells leads to highly efficient transformation, as evidenced by macroadenoma formation, within eight days following Cre induction (Barker et al., 2009), suggesting that loss of *Apc* is sufficient for transformation.

Here, we examine further the gatekeeping role of Apc by combining a conditional *Apc* allele (Apc^{CKO}) (Kuraguchi et al., 2006) with an out-of-frame *Cre* allele ($Pms2^{cre}$) that stochastically reverts back into frame (Miller et al., 2008). The $Pms2^{cre}$ mouse system used in this study is similar to cell type-specific conditional Cre/*lox* systems that model sporadic tumorigenesis by altering floxed genes in single cells surrounded by “normal” cells (Barker et al., 2009; Hung et al., 2010). However, in our system Cre activation occurs randomly throughout life without exogenous manipulations, therefore better mimicking the normal course of tumorigenesis. Moreover, multiple floxed alleles should be efficiently recombined within a single cell because the *Cre* allele should be constitutively expressed following frameshift mutation. The modified cell/cell lineage can be traced with a Cre-inducible marker gene, *R26R* (β-galactosidase or GFP), thus facilitating an assessment of the short- and longer-term consequences of target gene alteration. Because normal crypt stem cells are constantly replaced through neutral drift (Lopez-Garcia et al., 2010; Snippert et al., 2010), the mutated cell must compete with surrounding wild type stem cells to maintain crypt occupancy. By comparing clone sizes, it is possible to infer either negative selection (fewer or smaller $\beta\text{-gal}^+$ foci) or positive selection (more or larger $\beta\text{-gal}^+$ foci) conferred by specific mutation combinations even in the absence of morphologic changes.

The earliest phases of tumor progression are difficult to study because small tumors are easily overlooked, or may rapidly progress to larger tumors. Simplistically, loss of both *Apc* alleles should be sufficient to initiate intestinal tumorigenesis and lead to adenoma formation (Fearon and Vogelstein, 1990). In this study, combinations of different mutant *Apc* alleles reveal that the gatekeeper role of Apc is surprisingly complex because what we designate as “simultaneous” versus “stepwise” *Apc* loss yields different neoplastic phenotypes. Specifically, we have found that although simultaneous loss of both *Apc* alleles in otherwise Apc-normal intestines conferred a selective advantage (larger clone size), only a fraction of mutant cells became transformed. In contrast, we found that stepwise loss of *Apc*, in which Apc levels are compromised in the every cell of the mouse, resulted more often in overt transformation and adenoma formation.

RESULTS

Stochastic activation of Cre recombinase in the mouse small intestine

To study the consequences of targeted somatic mutation in single isolated cells, we developed a Cre-*lox* system in which recombination occurs in only a minority of intestinal crypts and is monitored by detection through expression of a Cre-reporter gene (Miller et al., 2008). Whole mount examination of *Pms2*$^{cre/cre}$*; Apc*$^{+/+}$*; Rosa-β-gal* mice at an average of 104 days revealed an average of 1845 β-gal^{+} foci in the proximal small intestine (Figure 1a). When sections were examined, we found that 2–3% of the crypts were β-gal^{+}, with 24% of the β-gal^{+} foci involving more than one crypt, suggesting that only a minority of Cre reversion events occur during development in control mice (Figures 1c and d, 2a and c). Furthermore, because the overall frequency of β-gal^{+} crypts is low, β-gal^{+} foci involving more than one crypt likely represent a single Cre-activation event followed by crypt fission rather than Cre-activation in adjacent crypts (<0.1% chance of independent adjacent crypt activation).

Stochastic loss of a single *Apc* allele in individual crypts

To determine if stochastic inactivation of one *Apc* allele detectably alters intestinal homeostasis, we combined the *Pms2*^{cre} allele with a conditional, floxed *Apc* allele, *Apc*^{CKO} (Kuraguchi et al., 2006). No microadenomas or adenomas were seen in the *Pms2*$^{cre/cre}$; *Apc*$^{CKO/+}$ mice (average age of 116 days). There were no significant differences in the numbers or sizes of β-gal^{+} patches between *Apc*$^{CKO/+}$ and *Apc*$^{+/+}$ mice (p=0.97 and p=0.46) (Figures 1a and b). However, the numbers of β-gal^{+} foci with staining of 3 adjacent villi were increased in *Apc*$^{CKO/+}$ mice compared to *Apc*$^{+/+}$ mice (p=0.01) (Figure 2e). Because a single crypt can contribute cells to typically at most 3 villi (Lopez-Garcia et al., 2010; Miller et al., 2008), the proportions of β-gal^{+} foci with 3 adjacent stained villi can serve as an indicator of crypts harboring a majority of recombined cells. Therefore, these results suggest that loss of a single *Apc* allele confers a selective advantage over adjacent wild type cells, more often leading to dominance within the crypt. However, this selective advantage is limited because somatic loss of only a single *Apc* allele did not detectably increase crypt fission (Figure 1d) or lead to transformation.

“Simultaneous” loss of both *Apc* alleles within individual crypts

Next, we examined *Pms2*$^{cre/cre}$; *Apc*$^{CKO/CKO}$; *Rosa-β-gal* mice to determine whether the simultaneous loss of both *Apc* alleles altered intestinal homeostasis. We use the term “simultaneous” in a relative sense to distinguish such somatic loss of both alleles within a single cell lineage from “stepwise” loss, in which one defective *Apc* allele is inherited followed by stochastic somatic loss of the remaining allele (see below). We realize that Cre recombination at the two *Apc*^{CKO} alleles in *Pms2*$^{cre/cre}$; *Apc*$^{CKO/CKO}$; *Rosa-β-gal* mice may occur over time in a particular cell lineage and not necessarily within the same cell cycle.

In contrast to *Apc*$^{+/+}$ or *Apc*$^{CKO/+}$ mice, *Apc*$^{CKO/CKO}$ mice developed anemia and were sacrificed at an average age of 114 days. Consistent with stochastic Cre-activation, β-gal^{+} foci were scattered throughout the intestines, with similar number of β-gal^{+} foci measured in both whole mount and sections when compared to either *Apc*$^{+/+}$ or *Apc*$^{CKO/+}$ mice (p=0.24

and p=0.97) (Figures 1a and c). However, the phenotypic consequences of simultaneous *Apc* loss were significantly different. As expected with complete *Apc* inactivation, β-gal$^+$ macroscopic adenomas were now present, with an average of 90 adenomas in the small intestine. In whole mount, ~4% of spots were scored as adenomas; however, smaller changes such as microadenomas are difficult to score when examining the intestine in whole mount. Therefore, to determine the percentage of abnormal β-gal$^+$ foci, we examined sections from the proximal small intestine. Interestingly, only 17% (22/129) of β-gal$^+$ foci in the proximal small intestine of *Apc*$^{CKO/CKO}$ mice were morphologically abnormal (microadenoma or adenoma) (Figure 3). However, there were other phenotypic consequences of simultaneous *Apc* loss in the absence of morphological transformation. Notably, *Apc*$^{CKO/CKO}$ mice had a significantly higher proportion of β-gal$^+$ foci involving either more than 3 villi or multiple adjacent crypts when compared to either *Apc*$^{+/+}$ or *Apc*$^{CKO/+}$ mice (p=0.02 and p=0.001) (Figures 1b and d, 2b and d). We note that the increased clonal expansion seen in *Apc*$^{CKO/CKO}$, but not in *Apc*$^{CKO/+}$ mice, supports efficient Cre recombination at both *Apc*^{CKO} alleles. These results demonstrate that simultaneous loss of both *Apc* alleles, likely occurring during intestinal development, confers additional selective advantages over surrounding wild type cells, but separates clonal expansion from transformation. Clonal expansion, manifested by crypt fission (larger β-gal$^+$ patches), without transformation was as common as clonal expansion with morphologic transformation.

Apc target alleles are efficiently recombined in β-gal$^+$ foci

In principle, Cre expression following frameshift reversion should result in efficient recombination of multiple *floxed* alleles because Cre expression should persist. As pointed out above, the increased crypt fission in *Apc*$^{CKO/CKO}$ but not in *Apc*$^{CKO/+}$ mice supports efficient recombination at both alleles. Nevertheless, the low percentage of β-gal$^+$ foci in the *Pms2*$^{cre/cre}$; *Apc*$^{CKO/CKO}$; *Rosa-β-gal* mice showing morphologic transformation might be explained by inefficient recombination of both *Apc*^{CKO} alleles. To verify Cre recombination efficiency, we used laser capture microdissection (LCM) on tissue cross sections to isolate β-gal$^+$ cells from normal appearing crypts or adenomas (Figures 4a–c). Next, we used quantitative PCR to measure the relative proportions of the recombined versus unrecombined *Apc*^{CKO} allele in microdissected samples enriched for β-gal$^+$ cells (Figure 4d). As expected, β-gal$^+$ adenomas showed significant enrichment for the recombined allele compared to β-gal$^-$ and *Apc*$^{\Delta/CKO}$ samples (p<0.001). For morphologically normal β-gal$^+$ foci, 76% (16/21) showed a significant 6–10 fold increase in signal of the recombined *Apc* allele over β-gal$^-$ cells and a significant 2–3 fold increase over *Apc*$^{\Delta/CKO}$ cells (p<0.001 for both). Also, consistent with recombination of both *Apc* alleles in the normal appearing β-gal$^+$ crypts, the enrichment of the recombined *Apc* allele in normal appearing β-gal$^+$ tissue was similar to that found in adenoma tissue (p=0.85) (Figure 4e). These results show that *Apc*^{CKO} is efficiently recombined in at least 75% of morphologically normal β-gal$^+$ crypts suggesting that the majority of these normal appearing crypts are indeed *Apc*-deficient.

Characteristics of Cre-reporter$^+$ foci in *Apc*$^{CKO/CKO}$ mice

To further examine morphologically normal β-gal$^+$ or GFP$^+$ crypts**,** most of which are *Apc*-deficient, we measured Wnt-dependent signaling, apoptosis and differentiation. Following

Apc loss it is expected that: WNT signaling be activated as reported by β-catenin deregulation, apoptosis be increased as reported by TUNEL, and the villus cell marker alkaline phosphatase be eliminated (Sansom et al., 2004). As expected, all β-gal$^+$ or GFP$^+$ foci that were scored as adenomas or microadenomas showed deregulated β-catenin expression (Figures 5a, g–i), increased TUNEL staining (Figure 5b) and a lack of alkaline phosphatase (Figure 5c). However, these changes were not seen in morphologically normal β-gal$^+$ or GFP$^+$ crypts and villi. First, all normal appearing β-gal$^+$ or GFP$^+$ fociexamined (30/30) from *Apc$^{CKO/CKO}$* mice showed normal levels and localization of β-catenin (Figures 5d, j-l). Second, only 7% (4/56) of normal appearing β-gal$^+$ crypts had evidence of apoptosis, similar to the level of apoptosis in neighboring β-gal$^-$ crypts (54/1399) (X^2=1.2, p=0.28) (Figure 5e). Finally, 10/10 β-gal$^+$ villi examined expressed alkaline phosphatase, whereas all adenomas examined did not stain for alkaline phosphatase (Yate's X^2=7.9, p=0.005) (Figure 5f). These results illustrate further that when normal morphology is retained after simultaneous inactivation of both *Apc* alleles, the increased crypt dominance and fission is not accompanied by significant changes in β-catenin, apoptosis or differentiation.

Attempts to generate Pms2$^{cre/cre}$; Apc$^{580S/580S}$ mice

Previous studies by others suggested that isolated functional loss of both *Apc* alleles in mouse intestinal stem cells was sufficient for transformation (Akyol et al., 2008; Barker et al., 2009). However, these studies were performed with a different conditional *Apc* allele, *Apc^{580S}*, from the *Apc^{CKO}* allele used here in our study. For a more direct comparison of our findings with these other studies, we attempted to generate *Pms2$^{cre/cre}$; Apc$^{580/580S}$* mice. We first generated *Pms2$^{cre/+}$*; *Apc$^{580S/580S}$* and Pms2$^{cre/+}$; Apc$^{CKO/CKO}$ mice. Next, we performed Pms2$^{cre/+}$; Apc$^{580S/580S}$ × Pms2$^{cre/+}$; Apc$^{580S/580S}$ and Pms2$^{cre/+}$; Apc$^{CKO/CKO}$ × Pms2$^{cre/+}$; Apc$^{CKO/CKO}$ matings, which are expected to yield 1 in 4 mice being Pms2$^{cre/cre}$ and either Apc$^{580S/580S}$ or Apc$^{CKO/CKO}$. While we were able to generate mice homozygous for the Apc^{CKO} allele in the expected Mendelian ratios (1:2:1) (15 Pms2$^{+/+}$:35 Pms2$^{cre/+}$:14 Pms2$^{cre/cre}$) (Yate's X^2=0.35, p=0.84), we were unsuccessful in generating Pms2$^{cre/cre}$; Apc$^{580S/580S}$ mice (9 Pms2$^{+/+}$:22 Pms2$^{cre/+}$:0 Pms2$^{cre/cre}$) (Yate's X^2=9.9, p=0.007). In addition, other crosses designed to generate Pms2$^{cre/cre}$; Apc$^{580S/580S}$ mice, albeit at a lower expected frequency, also failed to yield the desired genotype.

The *Apc^{CKO}* allele is expressed at wild type levels

Previous studies have reported that the conditional *Apc^{580S}* allele is hypomorphic, even prior to Cre recombination (Buchert *et al.*, 2010; Shibata *et al.*, 1997). The *Apc* allele used here, *Apc^{CKO}* (Kuraguchi et al., 2006), when acted on by Cre results in the same deletion of exon 14 and truncation of Apc at amino acid 580. However, in the *Apc^{CKO}* allele, the neomycin cassette was removed via FLP recombination, whereas the *Apc^{580S}* allele retains the neomycin cassette, possibly accounting for its hypomorphic nature (Shibata et al., 1997). To determine the expression level of the *Apc^{CKO}* allele, we measured Apc RNA levels by quantitative Real-Time PCR (qRT-PCR). While the *Apc$^{580S/580S}$* small intestine expressed only 40% of wild type Apc RNA levels, in agreement with a previous estimate (Shibata et al., 1997), the *Apc$^{CKO/CKO}$* small intestine expressed 101% of wild type Apc RNA levels (Table 1). In addition, whereas *Apc$^{CKO/Min}$* mice are viable (see below), *Apc$^{580S/Min}$* mice

die *in utero*, presumably due to significantly reduced overall Apc levels (Buchert et al., 2010). We conclude that the inability to generate *Pms2*$^{cre/cre}$; *Apc*$^{580S/580S}$ mice described above is also due to embryonic lethality.

"Stepwise" *Apc* loss results in more efficient transformation

The surprising finding that simultaneous *Apc* loss, when starting from normal Apc expression levels, frequently leads to clonal expansion (crypt fission) without morphologic transformation led us to use our system to determine the consequence of stepwise *Apc* loss, in which overall levels of Apc are reduced prior to complete *Apc* loss. We combined the *Apc*^{CKO} allele with one of two germline *Apc* mutations, *Apc*^{Min} or *Apc*^{1638N}. The *Min* allele, expressing a protein truncated at amino acid 850, results in ~50 adenomas at 6 months of age (Moser et al., 1990) (data not shown). The *1638N* allele results in truncation at amino acid 1638, is hypomorphic (~2% of wt) and predisposes to ~10 adenomas at 9 months of age (Smits et al., 1998) (data not shown). These two germline *Apc* alleles mimic the two different forms of FAP, normal and attenuated, based on differences in adenoma burden and onset of anemia.

Both *Apc*$^{Min/CKO}$ and *Apc*$^{1638N/CKO}$ mice became anemic at ~60 days of age, significantly more rapidly than the 114 days for *Apc*$^{CKO/CKO}$ mice ($p<0.001$) (Figure 6a). *Apc*$^{Min/CKO}$ mice had an average number of 171 adenomas in the small intestine, a significant increase ($p=0.01$) relative to *Apc*$^{CKO/CKO}$ mice. *Apc*$^{1638N/CKO}$ mice had an average of 225 adenomas in the small intestine, significantly more than *Apc*$^{CKO/CKO}$ mice ($p=0.00002$), but not significantly different from *Apc*$^{Min/CKO}$ mice ($p=0.11$) (Figure 6b). The percentage of β-gal^{+} cells in adenomas was similar between all three genotypes (*Apc*$^{CKO/CKO}$, *Apc*$^{Min/CKO}$ and *Apc*$^{1638N/CKO}$) ($X^2=4.2$, $p=0.4$), but different from *Apc*$^{1638N/+}$ mice ($X^2=132.4$, $p<0.001$), suggesting that Cre recombination is responsible for adenoma formation (Figure 7). Examination of the proximal small intestine cross sections revealed that 82% (47/57) and 88% (50/57) of β-gal^{+} foci in the *Apc*$^{Min/CKO}$ and *Apc*$^{1638N/CKO}$ mice, respectively, were scored as either a microadenoma or adenoma, indicating a significant five-fold increase when compared to *Apc*$^{CKO/CKO}$ mice ($X^2=72.5$, $p<0.001$ and $X^2=83.2$, $p<0.001$) (Figure 3). Nearly all crypts (>80%) undergo transformation after stepwise loss of *Apc*, which is in marked contrast to the minority of crypts (<20%) that undergo transformation after simultaneous *Apc* loss, in which overall Apc levels are normal. We propose based on the contrasting "simultaneous" versus "stepwise" results reported here that the overall Apc landscape can influence the consequences of *Apc* loss.

DISCUSSION

Progression to cancer is thought to occur through the acquisition of somatic changes associated with increasingly larger and more dysplastic precancerous lesions. Reconstruction of tumor progression is difficult because mutations can occur anywhere within the genome and serial observations are impractical. Human cancer genomes are difficult to interpret because they contain thousands of mutations. Most mutations are neutral "passenger" mutations and each cancer genome appears to be unique (Pleasance et al., 2010). For colorectal cancer, only a few genes (*APC, TP53, KRAS*) are mutated at

frequencies above 15% (Attolini et al., 2010; Forbes et al., 2010; Sjoblom et al., 2006). Consistent with the hypothesis that *APC* is a gatekeeper gene (Kinzler and Vogelstein, 1996), *APC* mutations are found in many human colorectal cancers and are the most common mutation in adenomas (Forbes et al., 2010).

Mouse models facilitate testing of the specific roles of certain mutations, either in a familial, or germline, context, or with conditional models that create specific mutations sometime after birth. Here, we use the *Pms2*^{cre} mouse system, which models several aspects of sporadic tumorigenesis, namely that mutations can occur anytime after conception, do not require external manipulations, and altered cells are initially isolated and surrounded by unaltered cells (Miller et al., 2008). In this system, Cre-mediated *Apc* deletion occurs stochastically in single isolated cells throughout life, induced by mutational slippage of an out-of-frame *cre* allele. The *Pms2*$^{cre/cre}$ mice used in this study are DNA mismatch repair (MMR) compromised, resulting in an increased rate of *Cre* reversion. The increased *Cre* reversion rate allowed us to achieve an optimal number of tumors by 4 months of age. Granted, MMR deficiency could have other consequences. However, because the control (those without conditional *Apc* alleles) and experimental mice (those with conditional *Apc* alleles) contain the same MMR defect, any consistent differences between the groups of mice should be due to the presence of the conditional alleles.

Using the *Pms2*^{cre} system, we examined the consequences of “simultaneous” versus “stepwise” *Apc* loss. What we define as simultaneous *Apc* loss, in which Apc levels are normal prior to *Apc* loss, resulted in increased crypt fission, but only 17% of β-gal^{+} crypts exhibited phenotypic dysplasia, i.e. adenoma formation and deregulated β-catenin expression. In contrast, we found that stepwise *Apc* loss, in which partial *Apc* deficiency due to an inherited mutation was followed by stochastic somatic *Apc* loss, resulted in >80% phenotypic dysplasia, consistent with other studies (Akyol et al., 2008; Barker et al., 2009). Our findings reveal that the gatekeeper role of Apc is surprisingly complex because simultaneous *Apc* loss had different phenotypic consequences than stepwise *Apc* loss. One could say, based on our findings, that the gate can open in two steps and that the gatekeeper role of Apc can be divided into two parts---net cell proliferation and morphologic transformation.

A notable difference between ours and another mouse study, which found essentially 100% tumorigenesis after induced homozygous *Apc* loss (Barker et al., 2009), is that the conditional *Apc* allele, *Apc*^{580S}, used in that study is hypomorphic, based on lower than wild type expression prior to Cre recombination (Buchert et al., 2010). In contrast, we have shown that the *Apc*^{CKO} allele used here expresses *Apc* at a level similar to wild type. Therefore, the use of the *Apc*^{CKO} allele allows us to uniquely engineer the loss of *Apc* in single, isolated cell lineages in mice with an otherwise normal Apc landscape. Our results show that inheriting an *Apc* defect (“one-hit”) fosters increased transformation upon somatic *Apc* loss, whereas simultaneous somatic *Apc* loss, in which overall Apc levels are normal prior to loss, frequently conferred clonal expansion through increased crypt fission, but did not necessarily result in morphologic transformation.

Although we believe that differences in overall Apc levels prior to *Apc* loss are important and can account for the contrasting results between our study and that of Barker *et. al.*, the two Cre/*lox* systems employed do have some other relevant differences. The *Lgr5-CreER* mouse model (Barker *et al.*, 2009) utilizes a single, low dose of tamoxifen to induce Cre recombination. Therefore, *Apc* loss occurs at a fixed point in time and likely within a limited time frame. Although both the $Pms2^{cre}$ and *Lgr5-CreER* systems resulted in a similar percentage of *Apc*-deficient (β-gal$^+$) crypts, it is possible that the slow accumulation of $Apc^{-/-}$ cells occurring in $Pms2^{cre}$ mice, as opposed to cells becoming $Apc^{-/-}$ within a limited time frame in the *Lgr5-CreER* mice is another contributing factor. Regardless, it will be important to compare the two different, conditional *Apc* alleles using the *Lgr5-CreER* system.

It is commonly presumed that $Apc^{-/-}$ cells are absent when visible intestinal lesions are not present. However, the occult presence of $Apc^{-/-}$ cells with normal morphologies rather than lack of mutation may better explain why chemoprevention with Sulindac in FAP patients initially causes polyp regression, but polyps subsequently reappear, with progression even to cancer (Cruz-Correa et al., 2002; Lynch, 2010). Rather than eliminating $Apc^{-/-}$ cells, visible regression with Sulindac may instead represent metaplastic conversion back to a normal histology. The presence or persistence of normal appearing $Apc^{-/-}$ cells would complicate surveillance efforts to prevent CRC.

The additional alterations required for morphologic transformation following simultaneous homozygous *Apc* loss are uncertain, but such changes may evolve more readily after stepwise loss of the first *Apc* allele. Notably, although $Apc^{+/-}$ intestines appear morphologically normal, their circuitry is altered because expression and proteomic profiles differ between $Apc^{+/+}$ and $Apc^{+/-}$ cells (Patel et al., 2011; Wang et al., 2010; Yeung et al., 2008). An acquired epigenetic mechanism or state present in $Apc^{+/-}$ cells, but not in $Apc^{+/+}$ cells, could modulate $Apc^{-/-}$ cell phenotypic plasticity. Supporting a requisite epigenetic role in transformation, polyp formation in Apc^{Min} mice is decreased when DNA methylation is inhibited (Eads et al., 2002; Laird et al., 1995), even though hypomethylation has been associated with both increased and decreased mutation rates (Chan et al., 2001; Chen et al., 1998). Alternatively $Apc^{-/-}$ cells may still arise in Apc^{Min} mice, but more often retain normal morphologies when DNA methylation is inhibited.

Our findings with simultaneous *Apc* loss in mice suggest that $Apc^{-/-}$ cells frequently retained a normal phenotype, thus raising the possibility that *Apc*-deficient cells could exist in the human colon and go undetected by conventional screening techniques. But *APC* is almost certainly lost in a stepwise fashion in human CRC, thus normal appearing, *APC*-deficient cells might be uncommon in the human colon. However, the Apc^{Min} and Apc^{1638N} alleles used to determine the consequences of stepwise loss of *Apc* are constitutive mutants, thus not only is Apc reduced in the cell that will become transformed upon *Apc* loss, but Apc levels are also reduced throughout the mouse. Thus, partial loss of Apc activity may lead to a more transformation-prone state due to cell autonomous effects such as abnormal spindle orientation (Quyn et al., 2010). Alternatively, there could be cell non-autonomous effects such as cross-talk between myofibroblasts and the epithelium (Quante *et al.*, 2011; Vermeulen *et al.*, 2010). Studies with stochastic *Apc* loss targeting specific cell types should

help distinguish between such explanations and elucidate further the important cell types involved in intestinal cancer.

The high frequency of *APC* mutations in human colorectal carcinomas indicates that APC function is usually lost during progression. The engineered isolated and simultaneous homozygous deletion of *Apc* in mice indicates that *Apc* loss can lead to clonal expansion but is usually insufficient for morphologic transformation. Our studies illustrate that the phenotypic plasticity observed in human cancers is also present very early in progression (Quintana et al., 2010). Further studies with different constellations of Cre-target genes can specifically test whether certain mutation combinations are sufficient for various stages of tumorigenesis. For example, using our system we found that *Kras* activation also resulted in clonal expansion without morphologic transformation (Miller et al., 2008). Potentially, the full malignant phenotype, including metastasis, can be engineered by Cre-mediated recombination of multiple oncogenes and/or tumor suppressor genes, thus facilitating specific testing of which combination(s) of pathway disruptions are necessary or sufficient for progression.

MATERIALS AND METHODS

Mice

Two different *R26R* (*Rosa26 Reporter* mice with either *lox-stop-lox LacZ* or *pCAGG lox-mTomato-lox mGFP*) alleles were used. Mice were housed in a specific pathogen free HEPA filtered room and were fed a diet of Purina PicoLab Rodent Diet 20.

Scoring of β-gal$^+$ foci in whole mount intestine

At least 20 β-gal$^+$ foci were counted for each third of the small intestine. Nearby β-gal$^+$ foci were considered independent if not arising from the same crypt and surrounded by non-staining crypts. Adenomas, which involved multiple villi, were scored by whole mount and in cross sections. Microadenomas, involving a single villus, were determined by scoring cross sections.

Laser capture microdissection of intestinal tissue for PCR

Sections were examined using an Arcturus^{XT} LCM instrument (Applied Biosystems) and β-gal$^+$ or β-gal$^-$ crypts/villi were attached to a CapSure Macro LCM Cap (Applied Biosystems) with an infrared laser. Band intensity was used to measure the relative ratio of recombined to unrecombined DNA (Quantity One, Bio-Rad). A sample known to contain a 1:1 ratio of recombined to unrecombined, run on each gel, was used to normalize against unknown samples.

Immunofluorescence

Sections were incubated in primary antibody (rabbit anti-β-catenin H-102, SantaCruz; TRITC-conjugated mouse anti-β-catenin, BD Transduction Labs; or rabbit anti-β-galactosidase, Immunology Consultants Laboratory) diluted 1:100 overnight at 4°C, washed in TBST then incubated in secondary antibody (anti-rabbit AlexaFluor 488, 555 or 633, Invitrogen) diluted 1:100 for 1 hour at RT.

Statistics

Data were analyzed with StatPlus for Mac in Microsoft Excel. Fisher LSD post-hoc test was used after ANOVA test. Chi^2 analysis was performed using a 2X2 or 2X3 Table.

Supplementary Material

Refer to Web version on PubMed Central for supplementary material.

Acknowledgments

We would like to thank Drs. James Stringer and Melissa Wong for critical reading of the manuscript. We also thank Drs. Raju Kucherlapati and Winfried Edelmann for the Apc^{CKO} and Apc^{1638N} mice, respectively, John Swain and Dr. Melissa Wong for Apc^{Min} mice and Apc^{580S} intestinal material and Dan Lioy and Drs. Gail Mandel and Paul Brehm for assistance with confocal microscopy. RML and DS were funded by NIH grant 2R01GM032741-28. JMF was funded by NIH training grant 5T32HD046420-05 and ACS postdoctoral fellow PF-11-067-01-TBE.

References

Akyol A, Hinoi T, Feng Y, Bommer GT, Glaser TM, Fearon ER. Generating somatic mosaicism with a Cre recombinase-microsatellite sequence transgene. Nat Methods. 2008; 5:231–3. [PubMed: 18264107]

Attolini CS, Cheng YK, Beroukhim R, Getz G, Abdel-Wahab O, Levine RL, et al. A mathematical framework to determine the temporal sequence of somatic genetic events in cancer. Proc Natl Acad Sci U S A. 2010; 107:17604–9. [PubMed: 20864632]

Barker N, Ridgway RA, van Es JH, van de Wetering M, Begthel H, van den Born M, et al. Crypt stem cells as the cells-of-origin of intestinal cancer. Nature. 2009; 457:608–11. [PubMed: 19092804]

Buchert M, Athineos D, Abud HE, Burke ZD, Faux MC, Samuel MS, et al. Genetic dissection of differential signaling threshold requirements for the Wnt/beta-catenin pathway in vivo. PLoS Genet. 2010; 6:e1000816. [PubMed: 20084116]

Chan MF, van Amerongen R, Nijjar T, Cuppen E, Jones PA, Laird PW. Reduced rates of gene loss, gene silencing, and gene mutation in Dnmt1-deficient embryonic stem cells. Mol Cell Biol. 2001; 21:7587–600. [PubMed: 11604495]

Chen RZ, Pettersson U, Beard C, Jackson-Grusby L, Jaenisch R. DNA hypomethylation leads to elevated mutation rates. Nature. 1998; 395:89–93. [PubMed: 9738504]

Cruz-Correa M, Hylind LM, Romans KE, Booker SV, Giardiello FM. Long-term treatment with sulindac in familial adenomatous polyposis: a prospective cohort study. Gastroenterology. 2002; 122:641–5. [PubMed: 11874996]

Eads CA, Nickel AE, Laird PW. Complete genetic suppression of polyp formation and reduction of CpG-island hypermethylation in Apc(Min/+) Dnmt1-hypomorphic Mice. Cancer Res. 2002; 62:1296–9. [PubMed: 11888894]

Fearon ER, Vogelstein B. A genetic model for colorectal tumorigenesis. Cell. 1990; 61:759–67. [PubMed: 2188735]

Fodde R, Edelmann W, Yang K, van Leeuwen C, Carlson C, Renault B, et al. A targeted chain-termination mutation in the mouse Apc gene results in multiple intestinal tumors. Proc Natl Acad Sci U S A. 1994; 91:8969–73. [PubMed: 8090754]

Forbes SA, Tang G, Bindal N, Bamford S, Dawson E, Cole C, et al. COSMIC (the Catalogue of Somatic Mutations in Cancer): a resource to investigate acquired mutations in human cancer. Nucleic Acids Res. 2010; 38:D652–7. [PubMed: 19906727]

Hung KE, Maricevich MA, Richard LG, Chen WY, Richardson MP, Kunin A, et al. Development of a mouse model for sporadic and metastatic colon tumors and its use in assessing drug treatment. Proc Natl Acad Sci U S A. 2010; 107:1565–70. [PubMed: 20080688]

Kinzler KW, Vogelstein B. Lessons from hereditary colorectal cancer. Cell. 1996; 87:159–70. [PubMed: 8861899]

Kuraguchi M, Wang XP, Bronson RT, Rothenberg R, Ohene-Baah NY, Lund JJ, et al. Adenomatous polyposis coli (APC) is required for normal development of skin and thymus. PLoS Genet. 2006; 2:e146. [PubMed: 17002498]

Laird PW, Jackson-Grusby L, Fazeli A, Dickinson SL, Jung WE, Li E, et al. Suppression of intestinal neoplasia by DNA hypomethylation. Cell. 1995; 81:197–205. [PubMed: 7537636]

Lopez-Garcia C, Klein AM, Simons BD, Winton DJ. Intestinal stem cell replacement follows a pattern of neutral drift. Science. 2010; 330:822–5. [PubMed: 20929733]

Lynch PM. Pharmacotherapy for inherited colorectal cancer. Expert Opin Pharmacother. 2010; 11:1101–8. [PubMed: 20345333]

Miller AJ, Dudley SD, Tsao JL, Shibata D, Liskay RM. Tractable Cre-lox system for stochastic alteration of genes in mice. Nature Methods. 2008; 5:227–229. [PubMed: 18264106]

Moser AR, Pitot HC, Dove WF. A dominant mutation that predisposes to multiple intestinal neoplasia in the mouse. Science. 1990; 247:322–4. [PubMed: 2296722]

Oshima M, Oshima H, Kitagawa K, Kobayashi M, Itakura C, Taketo M. Loss of Apc heterozygosity and abnormal tissue building in nascent intestinal polyps in mice carrying a truncated Apc gene. Proc Natl Acad Sci U S A. 1995; 92:4482–6. [PubMed: 7753829]

Patel BB, Li XM, Dixon MP, Blagoi EL, Nicolas E, Seeholzer SH, et al. APC +/− alters colonic fibroblast proteome in FAP. Oncotarget. 2011:2.

Pleasance ED, Cheetham RK, Stephens PJ, McBride DJ, Humphray SJ, Greenman CD, et al. A comprehensive catalogue of somatic mutations from a human cancer genome. Nature. 2010; 463:191–6. [PubMed: 20016485]

Quante M, Tu SP, Tomita H, Gonda T, Wang SS, Takashi S, et al. Bone marrow-derived myofibroblasts contribute to the mesenchymal stem cell niche and promote tumor growth. Cancer Cell. 2011; 19:257–72. [PubMed: 21316604]

Quintana E, Shackleton M, Foster HR, Fullen DR, Sabel MS, Johnson TM, et al. Phenotypic heterogeneity among tumorigenic melanoma cells from patients that is reversible and not hierarchically organized. Cancer Cell. 2010; 18:510–23. [PubMed: 21075313]

Quyn AJ, Appleton PL, Carey FA, Steele RJ, Barker N, Clevers H, et al. Spindle orientation bias in gut epithelial stem cell compartments is lost in precancerous tissue. Cell Stem Cell. 2010; 6:175–81. [PubMed: 20144789]

Sansom OJ, Reed KR, Hayes AJ, Ireland H, Brinkmann H, Newton IP, et al. Loss of Apc in vivo immediately perturbs Wnt signaling, differentiation, and migration. Genes Dev. 2004; 18:1385–90. [PubMed: 15198980]

Sasai H, Masaki M, Wakitani K. Suppression of polypogenesis in a new mouse strain with a truncated Apc(Delta474) by a novel COX-2 inhibitor, JTE-522. Carcinogenesis. 2000; 21:953–8. [PubMed: 10783317]

Shibata H, Toyama K, Shioya H, Ito M, Hirota M, Hasegawa S, et al. Rapid colorectal adenoma formation initiated by conditional targeting of the Apc gene. Science. 1997; 278:120–3. [PubMed: 9311916]

Sjoblom T, Jones S, Wood LD, Parsons DW, Lin J, Barber TD, et al. The consensus coding sequences of human breast and colorectal cancers. Science. 2006; 314:268–74. [PubMed: 16959974]

Smits R, van der Houven van Oordt W, Luz A, Zurcher C, Jagmohan-Changur S, Breukel C, et al. Apc1638N: a mouse model for familial adenomatous polyposis-associated desmoid tumors and cutaneous cysts. Gastroenterology. 1998; 114:275–83. [PubMed: 9453487]

Snippert HJ, van der Flier LG, Sato T, van Es JH, van den Born M, Kroon-Veenboer C, et al. Intestinal crypt homeostasis results from neutral competition between symmetrically dividing Lgr5 stem cells. Cell. 2010; 143:134–44. [PubMed: 20887898]

Su LK, Kinzler KW, Vogelstein B, Preisinger AC, Moser AR, Luongo C, et al. Multiple intestinal neoplasia caused by a mutation in the murine homolog of the APC gene. Science. 1992; 256:668–70. [PubMed: 1350108]

Vermeulen L, De Sousa EMF, van der Heijden M, Cameron K, de Jong JH, Borovski T, et al. Wnt activity defines colon cancer stem cells and is regulated by the microenvironment. Nat Cell Biol. 2010; 12:468–76. [PubMed: 20418870]

Wang D, Pezo RC, Corner G, Sison C, Lesser ML, Shenoy SM, et al. Altered dynamics of intestinal cell maturation in Apc1638N/+ mice. Cancer Res. 2010; 70:5348–57. [PubMed: 20570902]

Yeung AT, Patel BB, Li X-M, Seeholzer SH, Coudry RA, Cooper HS, et al. One-Hit Effects in Cancer: Altered Proteome of Morphologically Normal Colon Crypts in Familial Adenomatous Polyposis. Cancer Res. 2008; 68:7579–7586. [PubMed: 18794146]

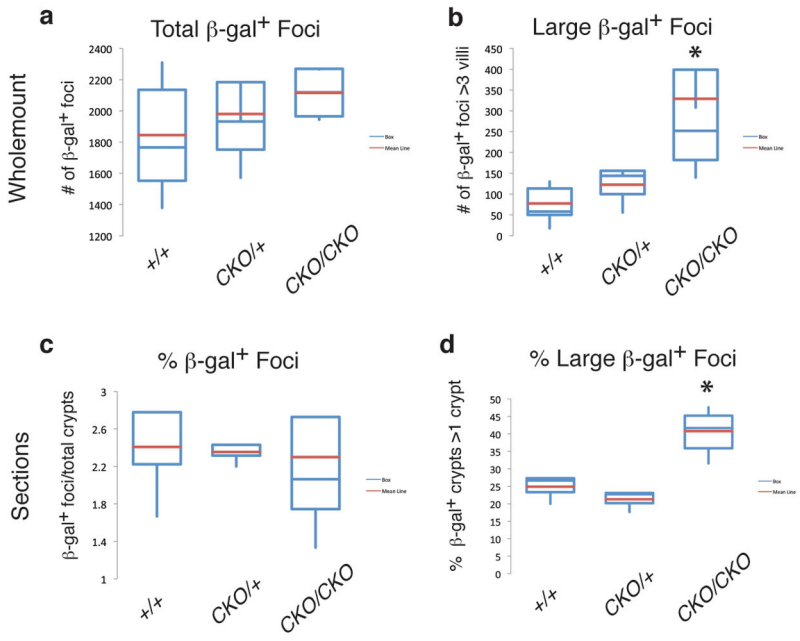

Figure 1. Increased crypt fission in *Apc*$^{CKO/CKO}$ mice

β-gal^{+} foci counted in whole mount (**a, b**), or sections of the proximal small intestine (**c, d**). (**a**) Note, there was no significant difference in the total number of β-gal^{+} foci between the three genotypes. (**b**) However, there was a significant increase in the number of "larger" β-gal^{+} foci, those involving more than three villi in *Apc*$^{CKO/CKO}$ mice (p=0.02). (**c**) In sections of the proximal small intestine, there was no significant difference in the percentage of β-gal^{+} foci. (**d**) In contrast, we did observe an increase in the percentage of β-gal^{+} foci involving more than one crypt in *Apc*$^{CKO/CKO}$ mice (p=0.001).

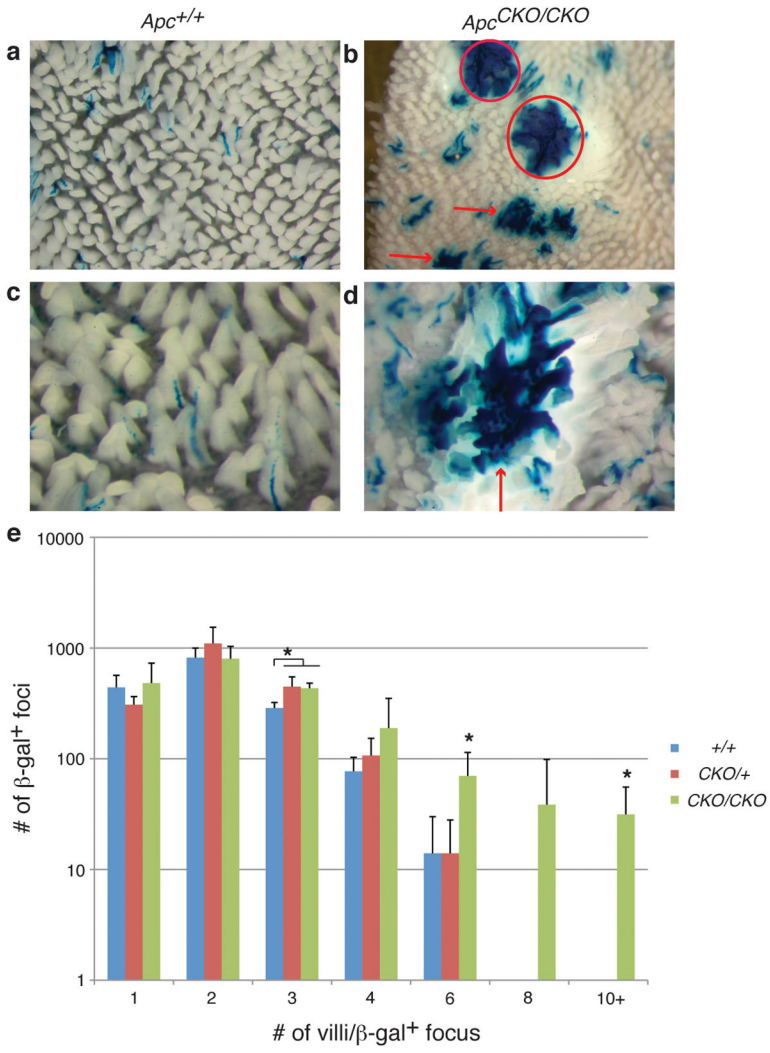

Figure 2. Increased number of larger β-gal$^+$ foci in *Apc$^{CKO/CKO}$* mice

(**a–d**) Whole mount images of proximal small intestine of *Apc*$^{+/+}$ and *Apc*$^{CKO/CKO}$ mice. Adenomas denoted with circles and larger normal β-gal$^+$ foci with arrows. (**b, d**) Images showing examples of larger normal β-gal$^+$ foci in *Apc*$^{CKO/CKO}$ mice. (**e**) Distribution of β-gal$^+$ foci sizes in the proximal small intestine of *Apc*$^{+/+}$, *Apc*$^{CKO/+}$ and *Apc*$^{CKO/CKO}$ mice. *Apc*$^{CKO/+}$ and *Apc*$^{CKO/CKO}$ mice show a significant increase in β-gal$^+$ foci involving 3 villi (p=0.01). *Apc*$^{CKO/CKO}$ show a significant increase in β-gal$^+$ foci involving 6 and 10 or more villi (p=0.02 and p=0.03, respectively).

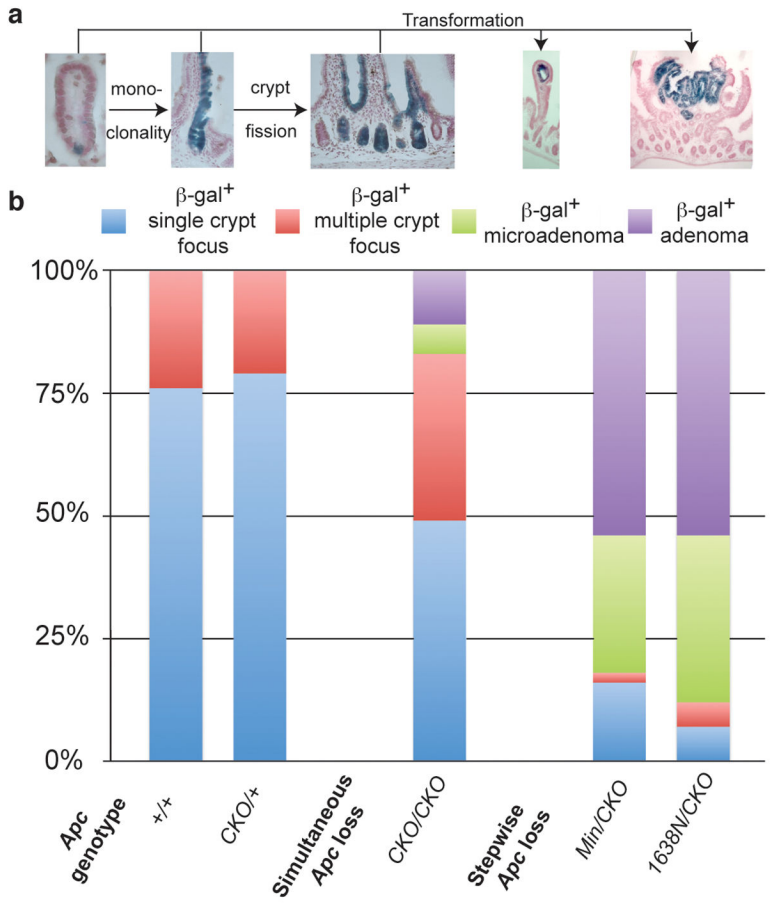

Figure 3. Distribution of normal and adenomatous β-gal$^+$ foci

(**a**) Images of different representative β-gal$^+$ foci illustrating a single β-gal$^+$ cell, single β-gal$^+$ crypt, multiple β-gal$^+$ crypts, β-gal$^+$ microadenoma and β-gal$^+$ adenoma. (**b**) Percentage of the β-gal$^+$ foci illustrated in (**a**).

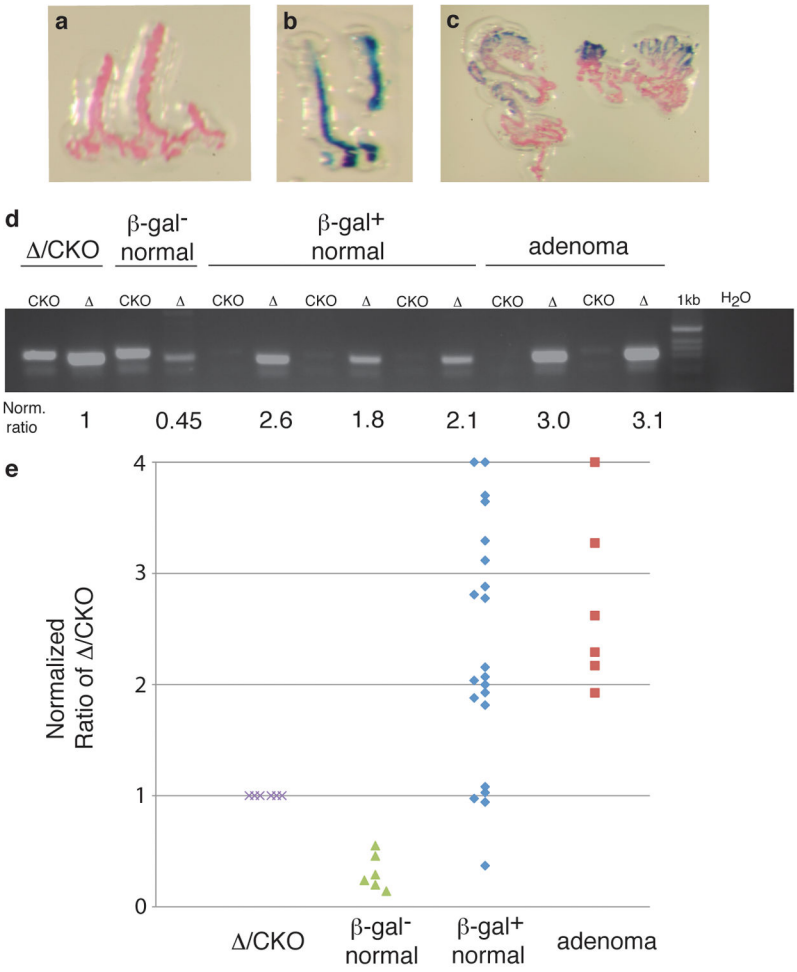

Figure 4. *Apc* is efficiently recombined in *Pms2*$^{cre/cre}$; *Apc*$^{CKO/CKO}$ mice

Images of (**a**) β-gal^{-} crypts, (**b**) β-gal^{+} crypts and (**c**) adenomas from the proximal small intestine isolated on LCM CAPs. (**d**) Gel of PCR reactions for the different isolated cell types. CKO is the unrecombined allele and Δ is the recombined allele. Each gel was normalized to the signal obtained from an *Apc*$^{\Delta/CKO}$ sample, which has a 1:1 ratio of recombined:unrecombined *Apc*^{CKO} alleles. (**e**) Graph of normalized recombined:unrecombined ratios that illustrates that 76% (16/21) of normal appearing β-gal^{+} samples had a 6–10 fold increase in the recombined:unrecombined ratio over β-gal^{-} cells ($p<0.001$), similar to the increase observed for the adenoma samples ($p=0.85$).

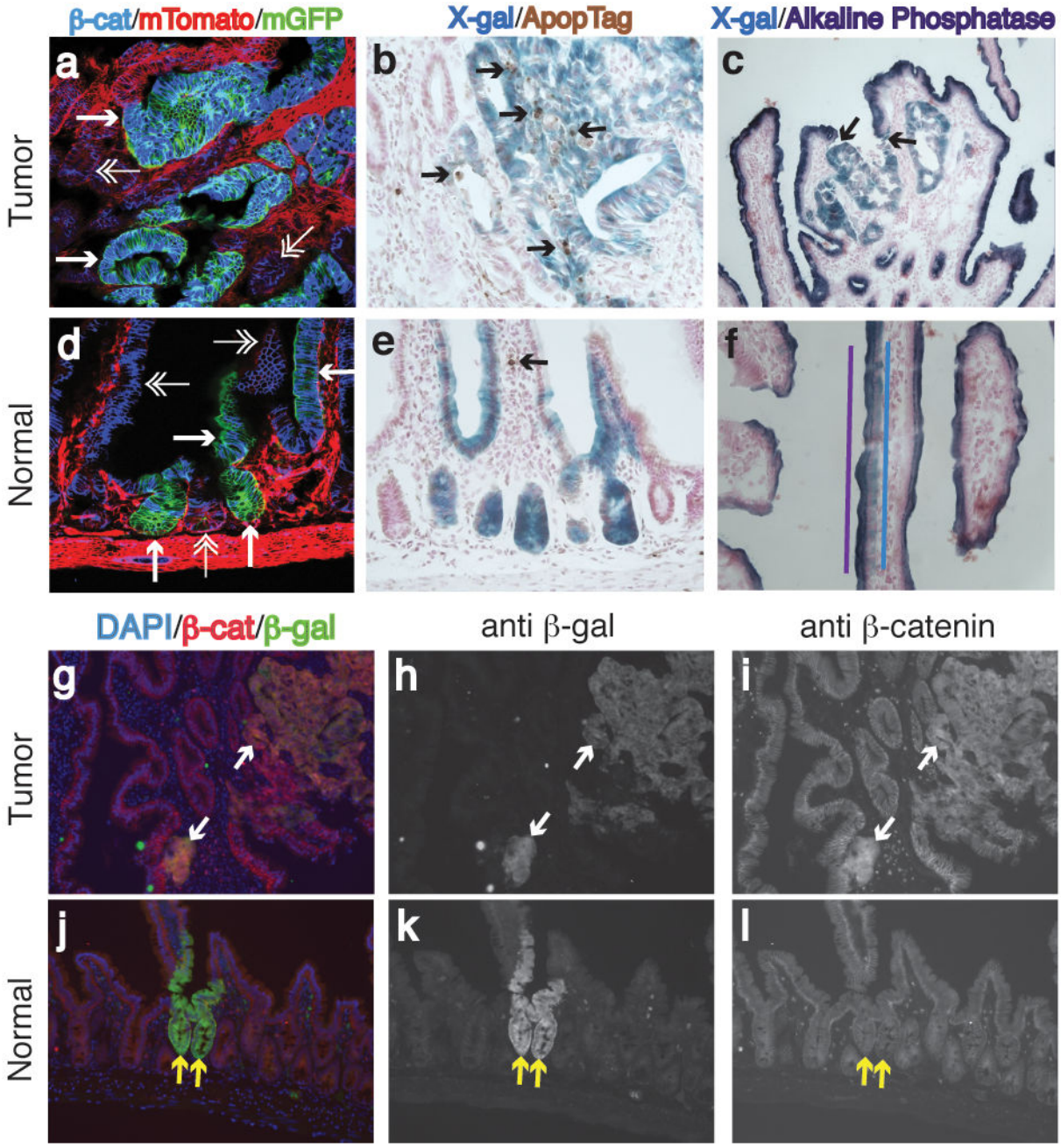

Figure 5. Characteristics of Cre-reporter$^+$ foci

Characterization of Cre-Reporter$^+$ tumor (**a–c, g–i**) and normal (**d–f, j–l**) tissue. (**a, d**) Show deregulated expression of β-catenin in GFP$^+$ tumor tissue (single arrowheads), but normal β-catenin expression in normal GFP$^+$ tissue (single arrowheads) (β-catenin:blue, mTomato:red[unrecombined], mGFP:green[recombined]). Double arrowheads point out unrecombined, epithelial tissue. (**b, e**) Show increased apoptosis in β-gal$^+$ tumor tissue, but normal apoptosis levels in normal, β-gal$^+$ tissue (β-gal$^+$:blue, TUNEL:brown). Arrows denote TUNEL positive cells. (**c, f**) Loss of alkaline phosphatase staining in β-gal$^+$ tumor tissue, but continued expression of alkaline phosphatase in normal, β-gal$^+$ tissue (β-

gal$^+$:blue, alkaline phosphatase:purple). In **c)** arrows show demarcation of alkaline phosphatase and X-gal staining. In **f)** purple and blue lines illustrate the overlap of alkaline phosphatase and β-gal$^+$ cells. (**g, j**) Merged images of immunofluorescence for β-catenin (red), β-gal (green) and DAPI (blue). Arrows point to the same β-gal$^+$ regions. (**h, k**) Shown are images of only the β-gal (green) channel. (**i, l**) Images of only the β-catenin (red) channel. Note, deregulated β-catenin expression n the tumor, but normal β-catenin pattern in the normal tissue.

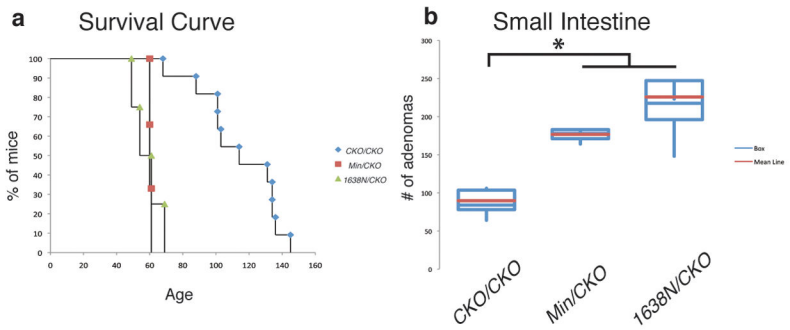

Figure 6. Increased tumor formation in $Apc^{Min/CKO}$ and $Apc^{1638N/CKO}$ mice

(**a**) Survival curve illustrating that $Apc^{Min/CKO}$ (red squares) and $Apc^{1638N/CKO}$ (green triangles) mice become anemic at an earlier age than $Apc^{CKO/CKO}$ (blue diamonds) mice ($p<0.001$). (**b**) Increased number of small intestinal adenomas in $Apc^{Min/CKO}$ and $Apc^{1638N/CKO}$ mice compared to $Apc^{CKO/CKO}$ mice ($p=0.01$).

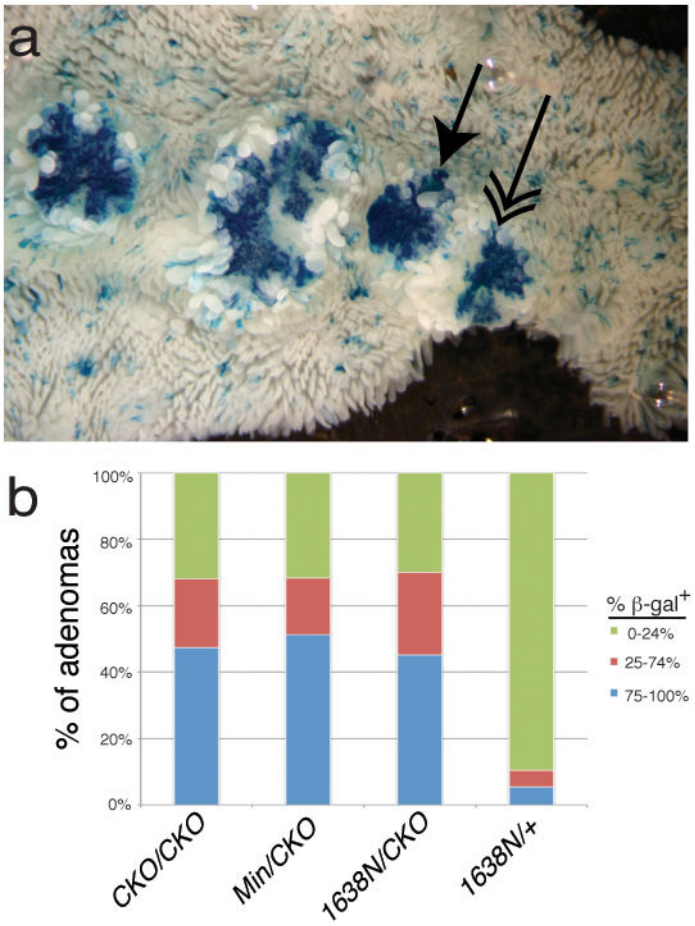

Figure 7. Percentage of β-gal$^+$ cells in proximal small intestine adenomas

(**a**) Whole mount image of β-gal$^+$ adenomas in *Apc*$^{CKO/CKO}$ mice. Single-headed arrow shows a tumor scored as 100% β-gal$^+$. Double-headed arrow shows a tumor scored as 50% β-gal$^+$. (**b**) Classification of adenomas into % β-gal$^+$ in the proximal small intestine.

Table 1

Quantitative Real Time PCR for Apc expression levels in the small intestine

	Apc	Actin and GAPDH			
	C_T	C_T	Δ C_T	ΔΔ C_T	% $Apc^{+/+}$
$Apc^{+/+}$	25.48	14.07	11.41	0	100
$Apc^{CKO/CKO}$	24.11	12.71	11.40	0.01	101
$Apc^{580S/580S}$	26.27	13.53	12.74	−1.33	40

C_T = cycle threshold (same threshold level of fluorescence for all samples)

$\Delta C_T = C_T$ (Apc) − C_T (actin and GAPDH)

$\Delta\Delta C_T = \Delta C_T$ ($Apc^{+/+}$) − ΔC_T ($Apc^{CKO/CKO}$ or $Apc^{580S/580S}$)

$\%Apc^{+/+} = 2^{\Delta\Delta Ct} \times 100$

Oncogene. Author manuscript; available in PMC 2012 October 19.